Environmental Science & Technology

pubs.acs.org/est

Article

Effect of Cu(II) on Mn(II) Oxidation by Free Chlorine To Form Mn Oxides at Drinking Water Conditions

Guiwei Li, Weiyi Pan, Lili Zhang, Ziqiao Wang, Baoyou Shi, and Daniel E. Giammar*

Cite This: *Environ. Sci. Technol.* 2020, 54, 1963−1972

Read Online

ACCESS | Metrics & More | Article Recommendations | Supporting Information

ABSTRACT: The chemical oxidation of dissolved Mn(II) to Mn(III/IV) oxides (MnO_x) can lead to the accumulation of Mn deposits in drinking water distribution systems. However, Mn(II) oxidation by free chlorine is quite slow under mild conditions (e.g., pH 7.7 and 1.0 mg/L Cl_2). This study found a significant role for Cu(II) in Mn(II) oxidation under conditions relevant to the supply of chlorinated drinking water. At pH 7.7, dissolved Cu(II) accelerated Mn(II) oxidation more than 10 times with a dose of 20 μg/L. Solid characterization revealed that during Mn(II) oxidation, Cu(II) adsorbed to freshly formed MnO_x and produced Mn−Cu mixtures (denoted as MnO_x−Cu(II)). An autocatalytic model for the reaction kinetics suggested that the freshly formed MnO_x−Cu(II) had a much higher catalytic activity than that of pure MnO_x. Solid CuO also catalyzed Mn(II) oxidation, and kinetic modeling indicated that after an initial oxidation of Mn(II) facilitated by the CuO surface, the freshly formed MnO_x−Cu(II) on CuO surface played the dominant role in accelerating further Mn(II) oxidation. This study indicates a high potential for the formation of Mn oxides at locations in a drinking water distribution system or in premise plumbing where both Mn(II) and Cu(II) are available. It provides insights into the co-occurrence of other metals with Mn deposits that is frequently observed in distribution systems.

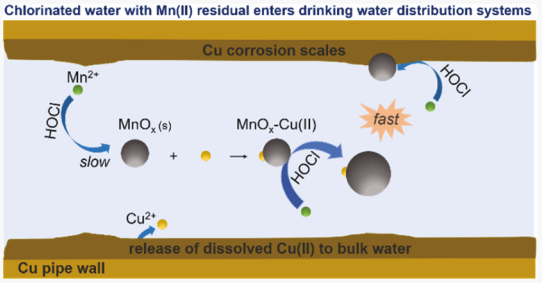

INTRODUCTION

Depending on its forms, Mn can cause aesthetic problems for drinking water at a concentration lower than a level that would cause adverse health effects.[1,2] Dissolved Mn(II) does not exhibit detectable taste nor color at tens of milligrams per liter.[3] It is particulate Mn(III/IV) oxides (MnO_x) that cause acceptability issues at concentrations less than 50 μg/L in drinking water. These issues include a detectable color and staining of laundry and plumbing fixtures.[3,4] MnO_x may also accumulate on the interior surface of water pipes and form Mn deposits that could later slough off under hydraulic disturbance and lead to "yellow water" or "black water" incidents.[5−9] Besides causing aesthetic issues, Mn in drinking water is often accompanied by various toxic metals and radionuclides,[10−16] suggesting potential health risks associated with Mn release together with co-occurring contaminants.

Dissolved Mn(II) is likely to enter drinking water distribution systems unless it is converted to a particulate form that can be removed by solid−liquid separation processes or it is taken up by a solid surface through sorption, ion-exchange, or biofiltration.[17−20] Under distribution system conditions, dissolved Mn(II) in finished water can form Mn particulates and deposits through either microbial or chemical pathways.[6,20,21] Microbially mediated formation of MnO_x was tightly related to the growth of Mn(II)-oxidizing bacteria on the surfaces of pipes where disinfectant residual was insufficient.[20,22−28] The chemical oxidation of Mn(II) by free chlorine is also important; large amounts of Mn deposits can be frequently found in distribution systems with good maintenance of free chlorine.[5,8,10] However, compared to stronger oxidants such as chlorine dioxide and ozone, free chlorine can only oxidize Mn(II) very slowly at near neutral pH.[29−33] Mn(II) oxidation can become autocatalytic once some initial MnO_x is formed; the main processes include the adsorption of Mn(II) to MnO_x and the subsequent oxidation of Mn(II) on the solid surface.[30,32,34] The following reactions can be used to describe the solution-phase and surface-catalyzed Mn(II) oxidation[32]

$$Mn^{2+} + HOCl + H_2O \xrightarrow{slow} MnO_2(s) + Cl^- + 3H^+ \quad (1)$$

$$MnO_2{\cdot}Mn^{2+}(s) + HOCl + H_2O \xrightarrow{accelerated} 2MnO_2(s) + Cl^- + 3H^+ \quad (2)$$

The speciation of chlorine and Mn(II) changes with pH (Figure S1). Here, the reactions are written with the main species present at pH 7; Mn^{2+} as the dominant Mn(II) species and HOCl as the representative form of free chlorine.

Received: October 28, 2019
Revised: December 20, 2019
Accepted: December 31, 2019
Published: January 14, 2020

Copper is another common element in drinking water. Typical levels of Cu in drinking water are below 1.3 mg/L (i.e., the USEPA action level). However, there are cases in which Cu can be problematic with a higher concentration.[35−37] The source of extra Cu is often the corrosion of Cu-bearing pipes and fittings (e.g., copper metal and brass) in service lines and premise plumbing.[38−40] The corrosion of copper and brass results in the oxidation of Cu(0) by free chlorine or dissolved oxygen to produce Cu(II) and Cu(I) that can be released to aqueous solution and incorporated into corrosion products that include malachite ($Cu_2CO_3(OH)_2$), tenorite (CuO), and cuprite (Cu_2O).[41−44]

In two drinking water distribution systems, Cu corrosion scales on brass components were found to be coated with large amounts of Mn deposits.[10] The co-occurrence of Mn and Cu is also supported by research conducted by Huang et al.[45] who found abundant Mn and Cu in deposits that accumulated inside cross-linked polyethylene pipe segments exhumed from household plumbing systems.[45] Further analysis of the deposit composition found a strong correlation (r^2 = 0.933) between Mn and Cu contents. The catalytic activity of the dissolved Cu(II) species and solid Cu(I/II) minerals have been reported for various reactions, including the degradation of iopamidol and the formation of trihalomethanes in distribution systems.[44,46−49]

This study was motivated by a need to better understand the mechanisms involved in the transformation of Mn(II) into MnO_x particulates in the presence of co-existing metals under conditions relevant to drinking water distribution. Considering the co-occurrence of Mn and Cu found in pipe deposits, this study aimed to identify the possible role of Cu(II) in the oxidation of Mn(II) by free chlorine. In pursuit of this objective, a series of batch experiments was conducted to study the reaction dynamics and the product characteristics in the absence and presence of Cu(II) species. Kinetic models of Mn(II) oxidation under different conditions were developed to help interpret the underlying mechanisms.

MATERIALS AND METHODS

Materials. Stock solutions (1.0 g/L) of dissolved Mn(II) and dissolved Cu(II) were prepared by dissolving manganese(II) sulfate monohydrate ($MnSO_4·H_2O$, Fisher Chemical) and copper(II) sulfate pentahydrate ($CuSO_4·5H_2O$, Fisher Scientific) in 1% HNO_3, respectively. Sodium hypochlorite (NaClO, Fisher Chemical) was used to prepare a free chlorine stock solution of 8.0 g/L (as Cl_2). Sodium thiosulfate ($Na_2S_2O_3$, Sigma-Aldrich) was used to prepare a 10.0 g/L stock solution. Commercially available copper(II) oxide powder (CuO, 99.995%) was purchased from Alfa Aesar. Dilute HNO_3 (0.1 M) and NaOH (0.1 M) were used for pH adjustment. All the solutions in this study were prepared with ultrapure water with a resistivity > 18.2 MΩ·cm.

Mn(II) Oxidation Experiments. Mn(II) oxidation experiments were conducted in the absence and presence of Cu(II). Dissolved Cu(II) (from dissolution of $CuSO_4$) and particulate CuO were investigated. Unless otherwise stated, all the experiments in this study were conducted at room temperature (24 ± 1 °C) and in duplicate with results presented as the mean ± standard deviation. Mn(II) and Cu(II) stock solutions and CuO solids were added to 1 L glass beakers to produce target concentrations. NaCl was added to gain a concentration of 1.0 mM in all solutions. In terms of dissolved inorganic carbon (DIC), the solutions in this study were in equilibrium with atmospheric CO_2 at different pH values. The calculated DIC concentrations in an open system were 0.07, 0.32, and 2.03 mM (Figure S2) at pH 7.0, 7.7, and 8.5, respectively. Predetermined amounts of $NaHCO_3$ were added to the initial solutions so that they would start closer to the DIC and pH values of an open system that were ultimately attained by pH adjustment with NaOH and equilibration with the atmospheric CO_2. Solution pH was maintained within 0.05 unit of that value by adding NaOH or HNO_3. An aliquot of chlorine stock solution was added to start the Mn(II) oxidation process. For the system with CuO, chlorine stock solution was dosed 4 h after the addition of Mn(II) and CuO. This was done to provide time for any initial adsorption of Mn(II) to the CuO particles and some release of dissolved Cu(II) from the CuO.

To avoid locally high pH or chlorine concentration, NaOH and chlorine were added under rapid magnetic agitation. As a typical regulatory level for Mn in finished water is in the range of 50−100 μg/L, a concentration of 100 μg/L (1.82 μM) was chosen as the initial Mn(II) dose in this study because this level occurs when there is poor Mn(II) removal, and it is within a concentration range of Mn(II) that can enter a distribution system. Solutions were highly undersaturated with respect to precipitation of $MnCO_3$ and $Mn(OH)_2$ solids (Figure S1). The 1.0 mg/L (14.1 μM) free chlorine dose was in excess of the amount needed for complete oxidation of 100 μg/L (1.82 μM) Mn(II).

During the process of Mn(II) oxidation, 10 mL water samples were collected periodically and filtered immediately. The samples were then acidified to contain 1% (w/w) HNO_3 for the analysis of the dissolved Mn and/or Cu concentration. Dissolved Mn was assumed to be the Mn(II) species that had not been oxidized to particulate MnO_x. Because a previous study found that MnO_x colloids (with a particle size < 0.22 μm) were formed from Mn(II) oxidation by chlorine,[29] centrifugal filters (Millipore, Amicon Ultra-15) with 10 kDa cut-off were selected to separate dissolved Mn(II) from colloidal MnO_x(s) in the Mn(II) oxidation experiments in the absence of added Cu(II). When either dissolved Cu(II) or CuO was added, the formed MnO_x particles were larger than 0.22 μm, so for these conditions, the 0.22 μm filters were suitable for determining the dissolved Mn. Dissolved Cu(II) was defined as Cu(II) that passed through 0.22 μm filters. We found that there was no difference in dissolved Cu(II) between samples filtered with 0.22 μm filters and with 0.05 μm filters.

15 mM of *tert* butyl alcohol (TBA, a common scavenger of hydroxyl radical) was dosed to the Mn(II) oxidation system with dissolved Cu(II). The rates of Mn(II) oxidation with and without TBA were compared to determine whether hydroxyl radical played a role in accelerating Mn(II) oxidation.[50,51]

Acidic Extraction of Cu(II) from Mn(II) Oxidation Products. Mn(II) oxidation in the presence of dissolved Cu(II) resulted in the uptake of Cu(II) by freshly formed solid phases. We denote the Cu(II)-bearing MnO_x as MnO_x−Cu(II). Experiments were designed to examine whether the Cu(II) was associated with MnO_x−Cu(II) through adsorption to the solid surface or incorporation within the structure of the solid. If the loss of dissolved Cu(II) during Mn(II) oxidation was because of Cu(II) adsorption to MnO_x, then the adsorbed Cu(II) could be easily desorbed at low pH.[52,53] After Mn(II) oxidation at a particular condition (pH 7.7, Mn(II) = Cu(II) = 100 μg/L, 1.0 mg/L Cl_2), 100 mL aliquots of the well-mixed suspension of MnO_x and Cu were transferred from the original beaker to 120 mL polypropylene bottles. The pH of each 100

https://dx.doi.org/10.1021/acs.est.9b06497
Environ. Sci. Technol. 2020, 54, 1963−1972

mL suspension was adjusted by addition of dilute HNO_3 to 7.0 ± 0.05, 5.0 ± 0.05, and 3.0 ± 0.05, respectively. The suspensions were magnetically stirred for 1.0 h to enable any desorption of Cu from the solids before samples were collected for the analysis of total (not filtered) and dissolved Cu and Mn concentrations. This experiment was conducted in duplicate.

Comparison of Catalytic Activities of MnO_x and MnO_x–Cu(II). In the Cu-free systems MnO_x was the only active substance that could catalyze Mn(II) oxidation. In the system containing dissolved Cu(II), the product of Mn(II) oxidation was hypothesized to be MnO_x–Cu(II) rather than pure MnO_x. To assess whether MnO_x and MnO_x–Cu(II) had different catalytic activities for Mn(II) oxidation, one experiment was performed with two rounds of Mn(II) oxidation. In the first round, Mn(II) oxidation was performed to prepare MnO_x suspensions with the same concentrations (as Mn) in the Cu(II)-free system and in the Cu(II)-containing system. The two systems were both at pH 7.7 ± 0.1 and initially contained 100 μg/L Mn(II), but only one system was dosed with 100 μg/L Cu(II). The Cu(II)-containing system contained a free chlorine concentration of 1.0 mg/L Cl_2 to oxidize Mn(II) for 4 h. In the Cu-free system, the free chlorine concentration was adjusted to 5.0 mg/L Cl_2 to accelerate the oxidation process to form MnO_x, and the reaction proceeded for 20 h. After the first-round oxidation was completed, the two systems both contained MnO_x solids with 100 μg/L as Mn in the overall suspension. To move on to the second round of the experiment, the free chlorine concentrations in each system were adjusted to 1.0 mg/L. For the Cu(II)-containing system, chlorine was supplemented by addition of sodium hypochlorite stock solution, while sodium thiosulfate stock solution was added to the Cu(II)-free system to quench excess chlorine. The amount of sodium thiosulfate added was such that its complete reaction lowered the free chlorine concentration to 1 mg/L Cl_2; consequently, the rapid consumption of thiosulfate essentially prevented its interaction with MnO_x. The second round oxidation of Mn(II) was then initiated by adding a fresh dose of 100 μg/L Mn(II) to the original reactors. The catalytic activities of MnO_x and MnO_x–Cu(II) for Mn(II) oxidation were compared based on the rates of this second round of Mn(II) oxidation.

Analytical Methods. The concentrations of Mn and Cu were determined by inductively coupled plasma mass spectrometry (PerkinElmer ELAN DRC II) with a detection limit of 0.1 μg/L. Standard samples of known concentrations were also measured at intervals for data quality control. The free chlorine concentration was measured with the DPD colorimetric method. Although MnO_x can potentially interfere with the DPD method, almost no MnO_x had formed at the time that samples were taken for measurement of free chlorine.[54] Zeta potential and particle size [based on dynamic light scattering (DLS) technique] were measured by a Malvern Zetasizer Nano ZS90 (Malvern Panalytical Ltd.) at room temperature. Transmission electron microscopy (TEM, Hitachi H-7500) was used to observe the size distribution of MnO_x particles. Scanning electron microscopy (SEM, FEI Nova NanoSEM 230) coupled with energy-dispersive X-ray spectroscopy (EDS) was used for the observation of particle size and morphology and for the elemental analysis of Mn oxides. Detailed methods for preparing SEM and TEM samples are provided in Supporting Information.

Model Development. For the reactions of Mn(II) under different conditions, different models were developed to aid in interpreting the decrease in dissolved Mn(II) concentration due to Mn(II) oxidation. The measured data were fitted to proposed kinetic models by minimizing the sum of squares (SS) (eq 3) of the difference between measured ($[Mn(II)]_{exp}$) and model-predicted concentrations ($[Mn(II)]_{fit}$) using the Solver function in Microsoft Excel.

$$SS = \sum_{i=1}^{n} ([Mn(II)]_{exp} - [Mn(II)]_{fit})^2 \quad (3)$$

Optimal values for the rate constants used in the kinetic model were obtained when SS was at a minimum. The rate equations used are provided in the following section.

RESULTS AND DISCUSSION

Mn(II) Oxidation by Free Chlorine. The oxidation of Mn(II) was a slow process when dissolved Mn(II) concentration, free chlorine dose, and pH were at levels most commonly encountered in distribution systems. As shown in Figure S3, about 10% of Mn(II) was oxidized by 1.0 mg/L Cl_2 within 12 h at pH 7.7. Compared to these mild conditions, either higher pH level (e.g., pH 8.5) or higher chlorine dose (e.g., 5 mg/L as Cl_2) would be required for faster Mn(II) oxidation. These observations are consistent with previous findings.[32,33]

Catalytic Effect of Dissolved Cu(II) on Mn(II) Oxidation. A dose of dissolved Cu(II) dramatically promoted Mn(II) oxidation (Figure 1). As compared to the Cu-free system, the amount of Mn(II) oxidized by free chlorine within 6 h increased more than 10 times in the presence of 20 μg/L Cu(II), a level quite attainable for distributed water. Increasing the Cu(II) concentration to 100 or 400 μg/L further accelerated Mn(II) oxidation.

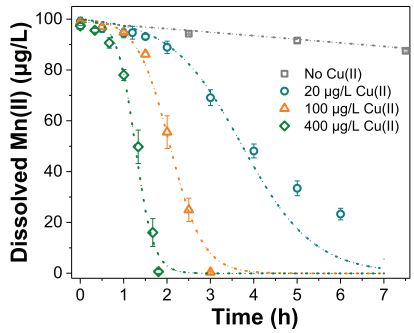

Figure 1. Catalytic effect of different concentrations of dissolved Cu(II) on the oxidation of 100 μg/L Mn(II) (1.82 μM). Experimental conditions: NaCl = 1.0 mM, Cl_2 = 1.0 mg/L (14.1 μM), pH = 7.7 ± 0.1, open to air. Dashed lines present the Mn(II) concentration predicted by the kinetic model. Error bars are the standard deviations of duplicate experiments.

Although the reaction rate was increased by Cu(II), a lag stage appeared before a stage of faster Mn(II) oxidation was observed. This pattern is typical of an autocatalytic process in which the accelerating stage of oxidation involves a product of the reaction acting as a catalyst for further reaction. In these experiments, the surface-catalyzed oxidation becomes predominant after the initial slow oxidation of Mn(II).[30,32] With the increase in Cu(II) dose, the lag time decreased, and the rapid stage of Mn(II) oxidation started sooner.

The kinetics of a typical surface-catalyzed Mn(II) oxidation can be written as the following rate expression (eq 4) and mole

https://dx.doi.org/10.1021/acs.est.9b06497
Environ. Sci. Technol. 2020, 54, 1963−1972

balance constraint (eq 5) based on the oxidation reactions (eqs 1 and 2) discussed previously[55]

$$\frac{d[Mn(II)]}{dt} = -k_0[Mn(II)] - k_{obs}[MnO_2][Mn(II)] \quad (4)$$

$$[MnO_2] = [Mn(II)]_0 - [Mn(II)] \quad (5)$$

Because in the Cu(II)-containing system the Mn(II) oxidation product was MnO_x–Cu(II) rather than pure MnO_x, the expression in eqs 4 and 5 can be rewritten as follows by replacing $[MnO_2]$ with $[MnO_x–Cu(II)]$

$$\frac{d[Mn(II)]}{dt} = -k_0[Mn(II)] - k_{obs}[MnO_x–Cu(II)]$$
$$[Mn(II)] \quad (6)$$

$$[MnO_x–Cu(II)] = [Mn(II)]_0 - [Mn(II)] \quad (7)$$

where k_0 is the first-order rate constant for homogeneous reaction and k_{obs} is the observed second-order rate constant for heterogeneous oxidation. k_0 depends on the oxidant concentration, pH, temperature, and Mn(II) speciation in solution while k_{obs} also depends on the nature of the MnO_x particulates.[56] The oxidant was stoichiometrically in large excess of the Mn(II) (14.1 μM Cl_2 vs 1.82 μM Mn(II)). Equation 7 accounts for Mn mass balance with $[Mn(II)]$ as the measured concentration of dissolved Mn(II) and $[Mn(II)]_0$ as the initial Mn(II) dose. To interpret the Mn(II) reaction rate when Cu(II) was added, a heterogeneous reaction model represented by eqs 6 and 7 was used. After variable separation, integration and transformation with details given by Wilson,[57] a function of Mn(II) concentration with time was derived from eqs 6 and 7

$$[Mn(II)] = \frac{k_0 + k_{obs}[Mn(II)]_0}{\frac{k_0}{[Mn(II)]_0} \cdot 10^{k_0 + k_{obs}[Mn(II)]_0/2.3 \cdot t} + k_{obs}} \quad (8)$$

The $[Mn(II)]$ calculated from eq 8 is then used as $[Mn(II)]_{fit}$ for finding the values of k_0 and k_{obs} that minimize the SS value in eq 3. For each of the systems with different concentrations of Cu(II) added (20, 100, and 400 μg/L), SS was calculated separately using eq 3 and denoted as SS_{20}, SS_{100}, and SS_{400}, respectively. The overall SS for the optimization of the data from experiments at all three Cu(II) concentrations was done as follows

$$\sum SS = SS_{20} + SS_{100} + SS_{400} \quad (9)$$

To minimize $\sum$SS, one k_0 value and three k_{obs} values (one for each of the three Cu(II) doses) were optimized simultaneously. The fitted k_0 value is 0.0114 h^{-1} and k_{obs} values were 0.0121, 0.0261, and 0.0475 $L \cdot \mu g^{-1} \cdot h^{-1}$ for the three systems, respectively. The model provided a good fit to the data (Figure 1) with goodness of fit (r^2) for the three Cu(II) concentrations being 0.967, 0.990, and 0.987, respectively. For the system containing 20 μg/L Cu(II) the last two points were not included in the fitting because they deviated greatly from the fitted line. For this system with low Cu(II), Cu(II) can become quickly depleted and the Mn(II) oxidation would likely not follow the same kinetic processes over the entire duration of the experiment.

Increasing pH increases the rate of homogeneous Mn(II) oxidation.[58] Figure 2 shows the effect of pH on Mn(II) oxidation in the presence of Cu(II). Compared with pH 7.7,

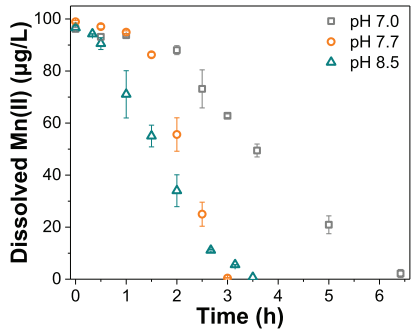

Figure 2. Effect of pH on Mn(II) oxidation by free chlorine in the presence Cu(II). Experimental conditions: NaCl = 1.0 mM, Mn(II) = 100 μg/L, Cu(II) = 100 μg/L, pH = 7.7 ± 0.1, Cl_2 = 1.0 mg/L, open to air. Error bars are the standard deviations of duplicate experiments.

Mn(II) oxidation proceeded at pH 7.0 but with a slower rate as expected. When pH was increased to 8.5, the lag time became shorter because of the faster homogeneous reaction.

However, at pH 8.5, after the initial stage the rate of Mn(II) oxidation was actually slower than at pH 7.7. It has been reported that CO_3^{2-} could form complexes with Mn^{2+} and slow Mn(II) oxidation.[59] At pH 7.7, the dominant dissolved Mn(II) species was Mn^{2+} (>96%, see Figure S1). Shifting the pH to 8.5 as an open system increased the proportion of $MnCO_3$(aq) species from 2% to about 56.4% (Mn^{2+} was 41.7%); the solution was undersaturated with respect to $MnCO_{3(s)}$. This change may have hindered the heterogeneous oxidation of Mn(II) by influencing the adsorption of Mn(II) to the solid surface and the formation of the adsorbed Mn(II) species.[30,60] In addition, the dominant dissolved Cu(II) species was different at pH 8.5 than at pH 7.7. When pH increased from pH 7.7 to 8.5, the proportion of HOCl species, which is a kinetically more potent oxidant than OCl^-, decreased from 40 to 10%. It was quite possible that the difference in Cu(II) and HOCl speciation also affected the Mn(II) oxidation rate.[30]

Formation of MnO_x–Cu(II). When Cu(II) was spiked into solutions to achieve a concentration of 20 or 100 μg/L at pH 7.7, almost all of the Cu(II) was dissolved (Figure S4). The dissolved species include Cu^{2+}, $CuOH^+$, and $CuCO_3$(aq) (Figure S5a). At 400 μg/L, dissolved Cu(II) was dominant, although Cu solids (about 60 μg Cu/L) started to precipitate. The solubility of $Cu(OH)_2$ at pH 7.7 is 350 μg/L (Figure S5b), a value quite close to the measured dissolved Cu(II) concentration with a 400 μg/L Cu(II) dose. The dissolved Cu(II) level was stable in a Mn(II)-free system (Figure S4). However, when Mn(II) and free chlorine were present, a dramatic decrease of dissolved Cu(II) concentration with time was observed (Figures 3 and S6). On the whole, the variation of dissolved Cu(II) concentration had the same trend as that of dissolved Mn(II) concentration. The oxidation of Mn(II) was associated with the "removal" of dissolved Cu(II) from solution.

The analysis of elemental composition of Mn oxidation products with EDS confirmed the uptake of Cu(II) by MnO_x. As shown in Figures S7 and S8, the MnO_x formed in the Cu(II)-containing system was a mixture of Mn and Cu. Notably, all particles included both Mn and Cu, and no particles were comprised of either entirely Mn or entirely Cu. Based on the SEM–EDS observations, the loss of dissolved Cu(II) during the Mn(II) oxidation process could be

https://dx.doi.org/10.1021/acs.est.9b06497
Environ. Sci. Technol. 2020, 54, 1963–1972

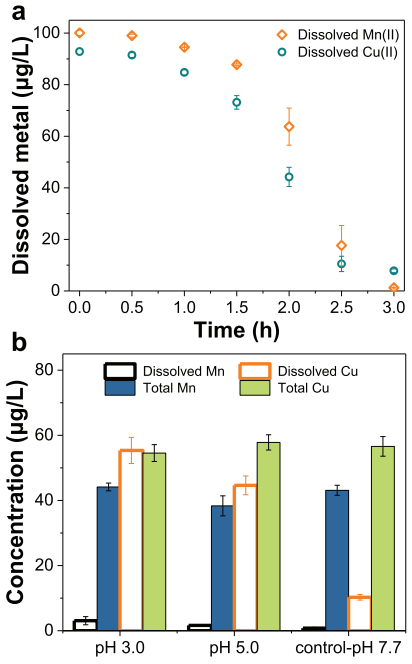

Figure 3. (a)Decrease of dissolved Cu(II) concentration during the oxidation of Mn(II) by free chlorine. Experimental conditions: NaCl = 1.0 mM, Cl_2 = 1.0 mg/L (14.1 μM), Cu(II) = 100 μg/L (1.56 μM), Mn(II) = 100 μg/L (1.82 μM), pH = 7.7 ± 0.1, open to air. (b) Release of dissolved Cu and Mn within 1 h after the adjustment of solution pH. Error bars are the standard deviations of duplicate experiments.

attributed to either Cu(II) adsorption to or incorporation into MnO_x.

Extraction experiments were conducted to examine if the Cu(II) that had been taken up by the newly formed solid phases could be released back to water phase under mildly acidic conditions.[61,62] In both the control system where the solution pH was maintained at 7.7 and in extractions at pH 3.0 and 5.0, the release of Mn to the water was negligible (Figure 3b). In contrast, the decrease of the pH from 7.7 to 5.0 released a large proportion (78%) of the Cu(II) to solution. A decrease to pH 3.0 released all of the Cu(II) to solution. As the release of Cu(II) was not accompanied by the dissolution of MnO_x, we deduce that the Cu(II) that was taken up by MnO_x during the oxidation of Mn(II) had accumulated as adsorbed and not structurally incorporated species. Adsorption of Cu(II) to MnO_x by inner-sphere complexation has been reported,[63,64] and the pH dependence of adsorption is consistent with previous studies.[65,66]

Catalytic Activities of MnO_x−Cu(II). In the Cu(II)-containing system, Mn(II) oxidation was dominated by a surface-catalysis mechanism. Based on the observed fast reaction in the Cu(II)-containing system, MnO_x−Cu(II) was hypothesized to be more active than pure MnO_x in catalyzing Mn(II) oxidation by free chlorine. The two-round Mn(II) oxidation experiments were designed to test this hypothesis. In the second round of oxidation, Mn(II) oxidation with MnO_x−Cu(II) present proceeded much faster than with pure MnO_x present (Figure 4).

As either MnO_x−Cu(II) or pure MnO_x was initially present in the two systems, there was no obvious lag time at the beginning of the reaction. The contribution of homogeneous oxidation of Mn(II) to overall Mn(II) oxidation was negligible.

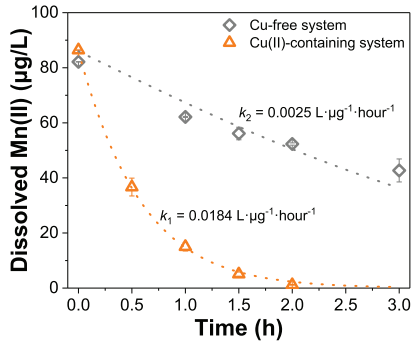

Figure 4. Second-round oxidation of Mn(II) by 1.0 mg/L of free chlorine in the solutions with 100 μg/L of MnO_x (1.82 μM) already formed from the first-round Mn(II) oxidation with and without 100 μg/L of Cu(II) (1.56 μM) present. Dashed lines present the Mn(II) concentration simulated by the kinetic model. Experimental conditions: NaCl = 1.0 mM, Cl_2 = 1.0 mg/L (14.1 μM), pH = 7.7 ± 0.1, open to air. Error bars are the standard deviations of duplicate experiments.

The rate equation of the second-round Mn(II) oxidation in the Cu(II)-containing system and in the Cu-free system could be written as eqs 10 and 11, respectively

$$\frac{d[Mn(II)]}{dt} = -k_1[MnO_x\text{−}Cu(II)][Mn(II)] - k_2[MnO_2][Mn(II)] \quad (10)$$

$$\frac{d[Mn(II)]}{dt} = -k_2([MnO_{2(first)}] + [MnO_2])[Mn(II)] \quad (11)$$

where k_1 and k_2 are the second-order rate constant for the heterogeneous oxidation catalyzed by MnO_x−Cu(II) and pure MnO_x, respectively. [MnO_x−Cu(II)] and [$MnO_{2(first)}$] are the concentrations of the first round Mn(II) oxidation products (100 μg/L, as Mn). [MnO_2] denotes the concentration of MnO_x newly formed in the second-round oxidation. These two kinetic models were successfully fit to interpret the decrease in dissolved Mn(II) concentration (Figure 4). The optimized k_1 and k_2 value were 0.0184 and 0.0025 L·μg^{-1}·h^{-1}, respectively. This result indicated that the catalytic activity of MnO_x−Cu(II) provided a rate constant 7.4 times as high as that from the catalytic activity of pure MnO_x. When the initial Cu(II) dose was 100 μg/L, k_1 in eq 10 and k_{obs} in eq 6 should be the same. The optimized k_{obs} in eq 6 (0.0261 L·μg^{-1}·h^{-1}) for the 100 μg/L-Cu(II) system was within 50% of the value of k_1 (0.0184 L·μg^{-1}·h^{-1}). The value of k_1 was probably slightly smaller than the k_{obs} value because of the coating of newly formed MnO_x on the outer surface of MnO_x−Cu(II) in the second round reaction.

The catalytic activity of a mineral can be inversely proportional to the particle size.[67,68] Although MnO_x−Cu(II) particles were larger than pure MnO_x particles (the results are shown in detail in the next section) and probably had lower specific surface area, their catalytic activity for Mn(II) oxidation was still much higher than that of pure MnO_x. This suggests that MnO_x−Cu(II) was inherently more reactive. Because Mn(II) oxidation was not fast at the initial stage where dissolved Cu(II) concentration was the highest (see Figure 1), we can conclude that the role of dissolved Cu(II) was not to initiate Mn(II) oxidation but to form

https://dx.doi.org/10.1021/acs.est.9b06497
Environ. Sci. Technol. 2020, 54, 1963−1972

MnO_x−Cu(II) particles that were then more catalytically active than pure MnO_x particles.

When there was continuous formation of MnO_x−Cu(II), Mn(II) oxidation was catalyzed by MnO_x−Cu(II), and the rate of Mn(II) oxidation could be simulated using the kinetic model developed by eqs 6 and 7 (Figure 1). However, if dissolved Cu(II) in the water phase was depleted, [MnO_x−Cu(II)] stopped increasing. The subsequent Mn(II) oxidation was catalyzed by both MnO_x−Cu(II) and MnO_x. For that scenario, eq 10, instead of eqs 6 and 7, is appropriate for predicting the Mn(II) oxidation rate. This can explain why the last two kinetic data of Mn(II) oxidation with 20 μg/L Cu(II) added (Figure 1) deviated from the output of the kinetic model developed from eqs 6 and 7; before Mn(II) oxidation was completed, the initial 20 μg/L Cu(II) had been completely consumed (Figure S6a), and the solid catalyzing further oxidation was no longer just MnO_x−Cu(II) but probably also some pure MnO_x. The premature slowdown of Mn(II) oxidation in the system with 20 μg/L Cu(II) also proved that the presence of dissolved Cu(II) and the continuous formation of MnO_x−Cu(II) were critical for fast Mn(II) oxidation.

Particle Size of Mn Oxides. Colloidal MnO_x (smaller than 0.22 μm) was formed as the oxidation product of Mn(II) with 5.0 mg/L free chlorine in the Cu-free system. The average size of MnO_x particulates determined by DLS was 120−200 nm (Figure 5a). TEM images further confirmed the formation of Mn colloids (Figure S9a). The measured zeta potential of the MnO_x suspensions was in the range of −8 to −18 mV (Figure S8b), consistent with previous studies showing that the Mn oxide surface was negatively charged because of the deprotonation of the surface hydroxyl groups.[69−71] Besides catalyzing Mn(II) oxidation, the addition of Cu(II) also made the oxidation product much larger (see SEM images in Figure S7). The average particle size of MnO_x in the Cu(II)-containing system determined by DLS was about 400 nm (Figure 5b). The results in Figure S10 show that dissolved Mn(II) concentrations in the Cu(II)-containing experiments as determined using 0.22 μm filters or 10 kDa filters were the same.

Because the zeta potential of Mn particles formed in the Cu(II)-containing system was the same as that of the particles in the Cu-free system (Figure S11), the different sizes of MnO_x in the two systems is probably not the result of neutralization of negative charge on MnO_x by Cu^{2+}. The different formation routes of MnO_x could be responsible for the difference in particle size. The particle size may have been larger in the systems with Cu(II) because of the continuous Mn(II) oxidation and Mn oxide growth on the surface of the seeds of MnO_x−Cu(II). In the Cu-free system, increasing chlorine concentration or pH did increase the rate of Mn(II) oxidation. However, because the pure MnO_x was not as active as MnO_x−Cu(II), increasing pH or chlorine concentration increased k_0 in eq 4 and consequently made the homogeneous oxidation of Mn(II) become more significant. In contrast, the surface catalytic reaction was the dominant mechanism in the systems with Cu(II).

Catalytic Effect of CuO on Mn(II) Oxidation. As a representative type of solid copper corrosion product, the effect of CuO on Mn(II) oxidation was explored. As shown in Figure 6a, the uptake of Mn(II) by 100 mg/L CuO was

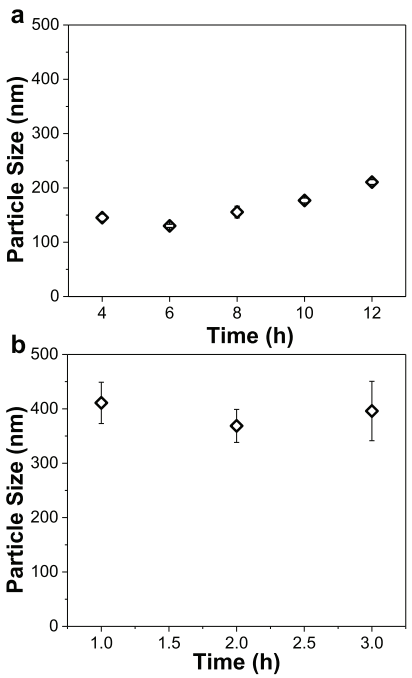

Figure 5. Particle size of MnO_x formed from the oxidation of Mn(II) (a) by 5.0 mg/L Cl_2 (70.4 μM) in the Cu-free system and (b) by 1.0 mg/L Cl_2 (14.1 μM) in the system containing 100 μg/L Cu(II) (1.56 μM). Other experimental conditions: NaCl = 1.0 mM, Mn(II) = 100 μg/L (1.82 μM), pH = 7.7 ± 0.1, open to air. Error bars are the standard deviations of triplicate measurements.

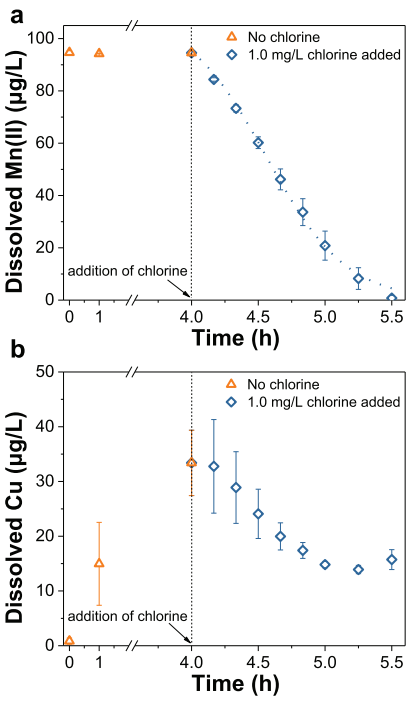

Figure 6. Change in (a) dissolved Mn(II) concentration and (b) dissolved Cu concentration before and after the addition of 1.0 mg/L (14.1 μM) free chlorine in the system containing both 100 mg/L CuO and 100 μg/L (1.82 μM) Mn(II). Other experimental conditions: pH 7.7 ± 0.1, NaCl = 1.0 mM, open to air. Dashed line presents the Mn(II) concentration simulated by the kinetic model for Mn(II) oxidation. Error bars are the standard deviations of duplicate experiments.

https://dx.doi.org/10.1021/acs.est.9b06497
Environ. Sci. Technol. 2020, 54, 1963−1972

negligible when there was no free chlorine present, suggesting a very limited Mn(II) adsorption capacity of CuO. The release of dissolved Cu(II) from 100 mg/L CuO within 4.0 h was less than 35 μg/L (Figure 6b). When 1.0 mg/L free chlorine was dosed to the system containing 100 mg/L CuO (denoted as CuO-containing system), the oxidation of 100 μg/L Mn(II) was completed within 1.5 h (Figure 6a), with a rate even faster than the reaction catalyzed by 400 μg/L Cu(II) (refer to Figure 1). This result suggested that, like dissolved Cu(II), solid CuO also had a catalytic effect on Mn(II) oxidation. No lag stage appeared in the CuO-containing system. After Mn(II) oxidation was initiated by the addition of free chlorine, the dissolved Cu(II) concentration started to decrease because of the uptake of dissolved Cu(II) (released by CuO) from solution. These observations of changing Cu(II) concentrations indicate that MnO_x−Cu(II) was also formed in the CuO-containing system. As shown by SEM−EDS results in Figure S12, the reaction product MnO_x was formed on the CuO surface.

Besides the catalytic effect of CuO itself, the newly formed MnO_x−Cu(II) also played an important role in promoting Mn(II) oxidation by free chlorine in the CuO-containing system. This is because the Mn(II) oxidation rate observed in Figure 6a did not decline even as Mn(II) concentration decreased, which indicates an autocatalytic process in which the reaction product (MnO_x−Cu(II)) is also promoting the reaction. As the homogeneous oxidation of Mn(II) was negligible, a rate equation together with eq 7 was developed to describe Mn(II) oxidation in the CuO-containing system:

$$\frac{\mathrm{d[Mn(II)]}}{\mathrm{d}t} = -k_1[\mathrm{CuO}][\mathrm{Mn(II)}] - k_2[\mathrm{MnO_x{-}Cu(II)}][\mathrm{Mn(II)}] \quad (12)$$

where k_1 and k_2 were the rate constants for the heterogeneous oxidation catalyzed by CuO and MnO_x−Cu(II), respectively. [CuO] was considered as a constant (100 mg/L). As shown in Figure 6a, the data could be fitted by this model very well (r^2 = 0.996). The optimized k_1 and k_2 were 4.4×10^{-6} and 0.0306 $(\mu g \cdot L^{-1} \cdot h)^{-1}$, respectively. When Mn(II) oxidation started in the CuO-containing system, the initial concentration of dissolved Cu(II) was about 30 μg/L. The value of k_2 was on the same order of magnitude as the value of 0.0261 $(\mu g \cdot L^{-1} \cdot h)^{-1}$ for k_{obs} in the system containing 100 μg/L of dissolved Cu(II). The slightly higher value of k_2 for the system with CuO solids could be because the aqueous solution may have been continuously supplemented with dissolved Cu(II) while the initial 100 μg/L Cu(II) was consumed in the experiment without CuO. Although the kinetics of Mn(II) oxidation in the CuO system could be interpreted well with MnO_x−Cu(II) as the catalytic species, we cannot rule out the possibility that MnO_x bound to CuO was the catalyst and that it was acting with a similar catalytic activity to the MnO_x−Cu(II) observed in the systems that started with dissolved Cu(II) and not CuO.

Temperature Dependence. The results shown in Figure S13 illustrate that even though Mn(II) oxidation was markedly promoted by the dissolved Cu(II) or CuO, the reaction could be significantly suppressed at a lower water temperature (15 °C). These results can be very useful to explain why Mn-related dirty water incidents are more common in summer.

Mechanism Discussion. The exact causes of the enhanced catalytic activity of MnO_x−Cu(II) are currently unknown. Some factors that may be related to the observed effect are noted below. In Mn(II) oxidation catalyzed by metal (oxyhydr)oxides, an electrochemical pathway was considered to be significant in which electron transfer occurred through the conduction band of the catalytic materials.[51] As reported, the introduction of transition metals into the framework of materials can bring about electronic property changes by creating defective microstructures.[72−74] The co-occurring metal cations can also change the properties of Mn oxides via adsorption above the vacancy sites of Mn oxides with layer or large tunnel structures.[75−79] For example, the adsorption of dissolved Cu(II) was found to alter the chemical structure and electronic properties of birnessite and its activity in a photo-induced reaction.[80] In this study, with the uptake of Cu(II), the Mn oxides formed in the Cu-containing system could have different properties from pure Mn oxides, which could associate with their different catalytic activities. To better understand the mechanism, future research could explore the catalyzed oxidation of Mn(II) on a broader range of metal-doped Mn oxides.

Another possibility was that highly reactive intermediate species formed in the system with both Cu(II) and free chlorine. As shown in Figure S14, the effect of Cu(II) on Mn(II) oxidation was not affected by the presence of TBA, indicating that the hydroxyl radical can be excluded from playing a role in the process. There are studies that identified the formation of Cu(III) as a potent oxidant and as an intermediate species in some systems.[81−84] It is possible that Cu(III) formed on the surface of MnO_x by the reaction with free chlorine. If MnO_x−Cu(III) was produced, then Mn(II) could be oxidized by Cu(III) rather than by free chlorine. The redox cycle between Cu(III) and Cu(II) could have contributed significantly to the enhanced Mn(II) oxidation, which would help explain the high catalytic activity of MnO_x−Cu(II) observed for Mn(II) oxidation.

Environmental Implications. As potential risks to drinking water supply, Mn deposits present challenges because they can be unpredictably re-suspended by water flow and spoil drinking water quality. However, the slow rate of Mn(II) oxidation under mild free chlorine and pH conditions could not explain why Mn deposits are frequently found on the interiors of pipe surfaces. This study addressed the significant role of Cu(II) in the transformation of soluble Mn(II) to form MnO_x solids under water chemistry conditions relevant to drinking water distribution. The results of this study can also explain the close association of Mn and Cu in pipe deposits. The findings suggest a high potential for accumulation of MnO_x deposits when Mn(II)-bearing water also contains Cu even at low concentrations.

Previous studies mainly focused on the catalytic effect of solid minerals on Mn(II) oxidation. We demonstrate that dissolved Cu(II) ions could also enhance Mn(II) oxidation by helping to form a solid of MnO_x that is catalytically more active. Future research can further explore the catalytic mechanisms by investigating the potential effects of other co-existing metals on Mn(II) oxidation and particulate formation. Such studies can help us understand why inorganic deposits in distribution systems are almost always a blend of various kinds of metals, such as Mn, Cu, Fe, Al, and Zn, and provide new insights into the control of Mn deposits.

https://dx.doi.org/10.1021/acs.est.9b06497
Environ. Sci. Technol. 2020, 54, 1963−1972

■ ASSOCIATED CONTENT

Supporting Information

The Supporting Information is available free of charge at https://pubs.acs.org/doi/10.1021/acs.est.9b06497.

Additional information about the TEM and SEM sample preparation; Figures of Mn(II) oxidation in the Cu-free system, particle size, TEM and SEM images, the distribution of dissolved Mn(II) and dissolved Cu(II) species, solubility of Mn(II) and Cu(II) minerals, decrease of dissolved Cu(II) concentration during the oxidation process of Mn(II), and effect of temperature on Mn(II) oxidation in the presence of Cu (PDF)

■ AUTHOR INFORMATION

Corresponding Author

Daniel E. Giammar − *Washington University in St. Louis, St. Louis, Missouri;* orcid.org/0000-0002-4634-5640; Email: giammar@wustl.edu

Other Authors

Guiwei Li − *Chinese Academy of Sciences, Beijing, China, Washington University in St. Louis, St. Louis, Missouri, and University of Chinese Academy of Sciences, Beijing, China*

Weiyi Pan − *Washington University in St. Louis, St. Louis, Missouri;* orcid.org/0000-0001-6587-1040

Lili Zhang − *Chinese Academy of Sciences, Beijing, China*

Ziqiao Wang − *Chinese Academy of Sciences, Beijing, China*

Baoyou Shi − *Chinese Academy of Sciences, Beijing, China, and University of Chinese Academy of Sciences, Beijing, China;* orcid.org/0000-0003-2129-4717

Complete contact information is available at: https://pubs.acs.org/10.1021/acs.est.9b06497

Notes

The authors declare no competing financial interest.

■ ACKNOWLEDGMENTS

This work was supported by the National Natural Science Foundation of China (51678558) and the U.S. National Science Foundation (CHE 1709484). G.L. acknowledges the international collaborative training scholarship rewarded by the University of Chinese Academy of Sciences. This work was performed in part using the Nanoscale Research Facility at Washington University in St. Louis, a member of the National Nanotechnology Infrastructure Network (NNIN), which was supported by the U.S. National Science Foundation under grant no. ECCS-0335765.

■ REFERENCES

(1) Harischandra, D. S.; Rokad, D.; Neal, M. L.; Ghaisas, S.; Manne, S.; Sarkar, S.; Panicker, N.; Zenitsky, G.; Jin, H.; Lewis, M.; Huang, X.; Anantharam, V.; Kanthasamy, A.; Kanthasamy, A. G. Manganese promotes the aggregation and prion-like cell-to-cell exosomal transmission of α-synuclein. *Sci. Signaling* **2019**, *12*, No. eaau4543.

(2) WHO. *Guidelines for Drinking-Water Quality*, 4th ed.; The World Health Organization: Geneva, 2011.

(3) Sain, A. E.; Dietrich, A. M. Rethinking aesthetic guidelines for manganese and iron in drinking water. *J. Water Supply: Res. Technol.–AQUA* **2015**, *64*, 775−782.

(4) Sain, A. E.; Griffin, A.; Dietrich, A. M. Assessing taste and visual perception of Mn (II) and Mn (IV). *J.—Am. Water Works Assoc.* **2014**, *106*, E32−E40.

(5) Li, G.; Ding, Y.; Xu, H.; Jin, J.; Shi, B. Characterization and release profile of (Mn, Al)-bearing deposits in drinking water distribution systems. *Chemosphere* **2018**, *197*, 73−80.

(6) Sly, L. I.; Hodgkinson, M. C.; Arunpairojana, V. Deposition of manganese in a drinking water distribution system. *Appl. Environ. Microbiol.* **1990**, *56*, 628−639.

(7) Waite, T.; Sly, L.; Khoe, G.; Dixon, D. R.; Chiswell, B.; Batley, G. Manganese and iron related problems in water supplies-Observations and research needs. *Australian Water and Wastewater Association 13th Federal Convention: Investing in Water Futures, the Australian Water Industry in the 1990's; Preprints of Papers, 1989*; Institution of Engineers: Australia, 1989; pp 437−440.

(8) Cerrato, J. M.; Reyes, L. P.; Alvarado, C. N.; Dietrich, A. M. Effect of PVC and iron materials on Mn (II) deposition in drinking water distribution systems. *Water Res.* **2006**, *40*, 2720−2726.

(9) Li, G.; Ma, X.; Chen, R.; Yu, Y.; Tao, H.; Shi, B. Field studies of manganese deposition and release in drinking water distribution systems: Insight into deposit control. *Water Res.* **2019**, *163*, 114897.

(10) Gerke, T. L.; Little, B. J.; Barry Maynard, J. Manganese deposition in drinking water distribution systems. *Sci. Total Environ.* **2016**, *541*, 184−193.

(11) Lytle, D. A.; Sorg, T.; Wang, L.; Chen, A. The accumulation of radioactive contaminants in drinking water distribution systems. *Water Res.* **2014**, *50*, 396−407.

(12) Copeland, R. C.; Lytle, D. A.; Dionysious, D. D. Desorption of arsenic from drinking water distribution system solids. *Environ. Monit. Assess.* **2007**, *127*, 523−535.

(13) Schock, M. R.; Cantor, A. F.; Triantafyllidou, S.; Desantis, M. K.; Scheckel, K. G. Importance of pipe deposits to Lead and Copper Rule compliance. *J.—Am. Water Works Assoc.* **2014**, *106*, E336−E349.

(14) Shi, Z.; Stone, A. T. PbO_2(s, Plattnerite) Reductive Dissolution by Aqueous Manganous and Ferrous Ions. *Environ. Sci. Technol.* **2009**, *43*, 3596−3603.

(15) Trueman, B. F.; Gregory, B. S.; McCormick, N. E.; Gao, Y.; Gora, S.; Anaviapik-Soucie, T.; L'Hérault, V.; Gagnon, G. A. Manganese Increases Lead Release to Drinking Water. *Environ. Sci. Technol.* **2019**, *53*, 4803−4812.

(16) Pan, W.; Pan, C.; Bae, Y.; Giammar, D. Role of Manganese in Accelerating the Oxidation of Pb(II) Carbonate Solids to Pb(IV) Oxide at Drinking Water Conditions. *Environ. Sci. Technol.* **2019**, *53*, 6699−6707.

(17) Tobiason, J. E.; Bazilio, A.; Goodwill, J.; Mai, X.; Nguyen, C. Manganese removal from drinking water sources. *Curr. Pollut. Rep.* **2016**, *2*, 168−177.

(18) Roccaro, P.; Barone, C.; Mancini, G.; Vagliasindi, F. G. A. Removal of manganese from water supplies intended for human consumption: a case study. *Desalination* **2007**, *210*, 205−214.

(19) Hamilton, G.; Chiswell, B.; Terry, J.; Dixon, D.; Sly, L. Filtration and manganese removal. *J. Water Supply: Res. Technol.–AQUA* **2013**, *62*, 417−425.

(20) Sly, L.; Hodgkinson, M.; Arunpairojana, V. The Control of Manganese Deposition and "Dirty Water" in the Gold Coast Water Distribution System. *Australian Water and Wastewater Association 13th Federal Convention: Investing in Water Futures, the Australian Water Industry in the 1990's; Preprints of Papers, 1989*; Institution of Engineers: Australia, 1989; pp 148−151.

(21) Dickinson, W. H.; Wiatr, C. Manganese-Related Corrosion and Fouling in Water Systems. *Analyst* **2013**, *20*, 20−35.

(22) Murdoch, F.; Smith, P. G. The interaction of a manganese-oxidising bacterium as part of a biofilm growing on distribution pipe materials. *Water Sci. Technol.* **2000**, *41*, 295−300.

(23) Murdoch, F.; Smith, P. G. Formation of manganese micro-nodules on water pipeline materials. *Water Res.* **1999**, *33*, 2893−2895.

(24) Sly, L. I.; Arunpairojana, V.; Dixon, D. R. Binding of colloidal MnO_2 by extracellular polysaccharides of Pedomicrobium manganicum. *Appl. Environ. Microbiol.* **1990**, *56*, 2791−2794.

(25) Sly, L. I.; Hodgkindon, M. C.; Arunpairojana, V. Effect of water velocity on the early development of manganese-depositing biofilm in a drinking-water distribution system. *FEMS Microbiol. Ecol.* **1988**, *53*, 175−186.
(26) Sly, L. I.; Arunpairojana, V.; Hodgkinson, M. C. Pedomicrobium manganicum from drinking-water distribution systems with manganese-related "dirty water" problems. *Syst. Appl. Microbiol.* **1988**, *11*, 75−84.
(27) Cerrato, J. M.; Falkinham, J. O., III; Dietrich, A. M.; Knocke, W. R.; McKinney, C. W.; Pruden, A. Manganese-oxidizing and-reducing microorganisms isolated from biofilms in chlorinated drinking water systems. *Water Res.* **2010**, *44*, 3935−3945.
(28) Linhardt, P. Manganese Oxides in Pipes of Galvanized Steel for Potable Water—A Potential Risk of MIC?. *Corrosion 2002*; NACE International: Denver, Colorado, 2002; pp 1−8.
(29) Li, G.; Hao, H.; Zhuang, Y.; Wang, Z.; Shi, B. Powdered activated carbon enhanced manganese(II) removal by chlorine oxidation. *Water Res.* **2019**, *156*, 287−296.
(30) Allard, S.; Fouche, L.; Dick, J.; Heitz, A.; Von Gunten, U. Oxidation of manganese (II) during chlorination: role of bromide. *Environ. Sci. Technol.* **2013**, *47*, 8716−8723.
(31) Van Benschoten, J. E.; Lin, W.; Knocke, W. R. Kinetic modeling of manganese (II) oxidation by chlorine dioxide and potassium permanganate. *Environ. Sci. Technol.* **1992**, *26*, 1327−1333.
(32) Hao, O. J.; Davis, A. P.; Chang, P. H. Kinetics of manganese (II) oxidation with chlorine. *J. Environ. Eng.* **1991**, *117*, 359−374.
(33) Knocke, W. R.; Hoehn, R. C.; Sinsabaugh, R. L. Using Alternative Oxidants to Remove Dissolved Manganese From Waters Laden With Organics. *J.—Am. Water Works Assoc.* **1987**, *79*, 75−79.
(34) Gregory, D.; Carlson, K. Effect of soluble Mn concentration on oxidation kinetics. *J.—Am. Water Works Assoc.* **2003**, *95*, 98−108.
(35) WHO. *Copper in Drinking-Water, Background Document for Development of WHO Guidelines for Drinking-Water Quality*, 2004.
(36) Georgopoulos, P. G.; Wang, S. W.; Georgopoulos, I. G.; Yonone-Lioy, M. J.; Lioy, P. J. Assessment of human exposure to copper: A case study using the NHEXAS database. *J. Exposure Sci. Environ. Epidemiol.* **2006**, *16*, 397−409.
(37) Dietrich, A. M.; Glindemann, D.; Pizarro, F.; Gidi, V.; Olivares, M.; Araya, M.; Camper, A.; Duncan, S.; Dwyer, S.; Whelton, A. J.; Younos, T.; Subramanian, S.; Burlingame, G. A.; Khiari, D.; Edwards, M. Health and aesthetic impacts of copper corrosion on drinking water. *Water Sci. Technol.* **2004**, *49*, 55−62.
(38) Palit, A.; Pehkonen, S. O. Copper corrosion in distribution systems: evaluation of a homogeneous Cu_2O film and a natural corrosion scale as corrosion inhibitors. *Corros. Sci.* **2000**, *42*, 1801−1822.
(39) Vargas, I. T.; Pavissich, J. P.; Olivares, T. E.; Jeria, G. A.; Cienfuegos, R. A.; Pastén, P. A.; Pizarro, G. E. Increase of the concentration of dissolved copper in drinking water systems due to flow-induced nanoparticle release from surface corrosion by-products. *Corros. Sci.* **2010**, *52*, 3492−3503.
(40) Xiao, W.; Hong, S.; Tang, Z.; Seal, S.; Taylor, J. S. Effects of blending on surface characteristics of copper corrosion products in drinking water distribution systems. *Corros. Sci.* **2007**, *49*, 449−468.
(41) Schock, M. R.; Lytle, D. A.; Clement, J. A. *Effect of pH, DIC, Orthophosphate and Sulfate on Drinking Water Cuprosolvency*; National Risk Management Research Laboratory: Cincinnati, OH, United States, 1995.
(42) Taxén, C.; Letelier, M. V.; Lagos, G. Model for estimation of copper release to drinking water from copper pipes. *Corros. Sci.* **2012**, *58*, 267−277.
(43) Merkel, T. H.; Groß, H.-J.; Werner, W.; Dahlke, T.; Reicherter, S.; Beuchle, G.; Eberle, S. H. Copper corrosion by-product release in long-term stagnation experiments. *Water Res.* **2002**, *36*, 1547−1555.
(44) Yuan, X.; Pham, A. N.; Miller, C. J.; Waite, T. D. Copper-catalyzed hydroquinone oxidation and associated redox cycling of copper under conditions typical of natural saline waters. *Environ. Sci. Technol.* **2013**, *47*, 8355−8364.
(45) Huang, X.; Pieper, K. J.; Cooper, H. K.; Diaz-Amaya, S.; Zemlyanov, D. Y.; Whelton, A. J. Corrosion of upstream metal plumbing components impact downstream PEX pipe surface deposits and degradation. *Chemosphere* **2019**, *236*, 124329.
(46) Hu, J.; Dong, H.; Qu, J.; Qiang, Z. Enhanced degradation of iopamidol by peroxymonosulfate catalyzed by two pipe corrosion products (CuO and δ-MnO_2). *Water Res.* **2017**, *112*, 1−8.
(47) Li, B.; Qu, J.; Liu, H.; Hu, C. Effects of copper (II) and copper oxides on THMs formation in copper pipe. *Chemosphere* **2007**, *68*, 2153−2160.
(48) Chen, J.; Sun, P.; Zhou, X.; Zhang, Y.; Huang, C.-H. Cu (II)−catalyzed transformation of benzylpenicillin revisited: the overlooked oxidation. *Environ. Sci. Technol.* **2015**, *49*, 4218−4225.
(49) Ahmad, J. U.; Räisänen, M. T.; Leskelä, M.; Repo, T. Copper catalyzed oxidation of benzylic alcohols in water with H_2O_2. *Appl. Catal., A* **2012**, *411−412*, 180−187.
(50) Li, X.; Li, J.; Bai, J.; Dong, Y.; Li, L.; Zhou, B. The Inhibition Effect of Tert-Butyl Alcohol on the TiO_2 Nano Assays Photoelectrocatalytic Degradation of Different Organics and Its Mechanism. *Nano-Micro Lett.* **2016**, *8*, 221−231.
(51) Lan, S.; Wang, X.; Xiang, Q.; Yin, H.; Tan, W.; Qiu, G.; Liu, F.; Zhang, J.; Feng, X. Mechanisms of Mn(II) catalytic oxidation on ferrihydrite surfaces and the formation of manganese (oxyhydr) oxides. *Geochim. Cosmochim. Acta* **2017**, *211*, 79−96.
(52) Pagnanelli, F.; Esposito, A.; Toro, L.; Vegliò, F. Metal speciation and pH effect on Pb, Cu, Zn and Cd biosorption onto Sphaerotilus natans: Langmuir-type empirical model. *Water Res.* **2003**, *37*, 627−633.
(53) Yang, J. Y.; Yang, X. E.; He, Z. L.; Li, T. Q.; Shentu, J. L.; Stoffella, P. J. Effects of pH, organic acids, and inorganic ions on lead desorption from soils. *Environ. Pollut.* **2006**, *143*, 9−15.
(54) Clesceri, L. S.; Greenberg, A. E.; Eaton, A. D. *Standard Methods for the Examination of Water and Wastewater*, 20th ed.; American Public Health Association: Washington, DC, 1998.
(55) Kessick, M. A.; Morgan, J. J. Mechanism of autoxidation of manganese in aqueous solution. *Environ. Sci. Technol.* **1975**, *9*, 157−159.
(56) Sigel, H. Manganese in natural waters and earth's crust: Its availability to organisms. *Metal Ions in Biological Systems*; CRC Press, 2000.
(57) Wilson, D. E. Surface and complexation effects on the rate of Mn (II) oxidation in natural waters. *Geochim. Cosmochim. Acta* **1980**, *44*, 1311−1317.
(58) Morgan, J. J. Kinetics of reaction between O_2 and Mn (II) species in aqueous solutions. *Geochim. Cosmochim. Acta* **2005**, *69*, 35−48.
(59) Hem, J. D. *Chemical Equilibria and Rates of Manganese Oxidation*; US Government Printing Office, 1963.
(60) Davies, S. H. R.; Morgan, J. J. Manganese (II) oxidation kinetics on metal oxide surfaces. *J. Colloid Interface Sci.* **1989**, *129*, 63−77.
(61) Gadde, R. R.; Laitinen, H. A. Heavy metal adsorption by hydrous iron and manganese oxides. *Anal. Chem.* **1974**, *46*, 2022−2026.
(62) McKenzie, R. The adsorption of lead and other heavy metals on oxides of manganese and iron. *Soil Res.* **1980**, *18*, 61−73.
(63) Sherman, D. M.; Peacock, C. L. Surface complexation of Cu on birnessite (δ-MnO_2): Controls on Cu in the deep ocean. *Geochim. Cosmochim. Acta* **2010**, *74*, 6721−6730.
(64) Peña, J.; Bargar, J. R.; Sposito, G. Copper sorption by the edge surfaces of synthetic birnessite nanoparticles. *Chem. Geol.* **2015**, *396*, 196−207.
(65) Rahnemaie, R.; Hiemstra, T.; van Riemsdijk, W. H. Inner- and outer-sphere complexation of ions at the goethite-solution interface. *J. Colloid Interface Sci.* **2006**, *297*, 379−388.
(66) Manceau, A.; Charlet, L.; Boisset, M. C.; Didier, B.; Spadini, L. Sorption and speciation of heavy metals on hydrous Fe and Mn oxides. From microscopic to macroscopic. *Appl. Clay Sci.* **1992**, *7*, 201−223.

https://dx.doi.org/10.1021/acs.est.9b06497
Environ. Sci. Technol. 2020, 54, 1963−1972

(67) Madden, A. S.; Hochella, M. F. A test of geochemical reactivity as a function of mineral size: Manganese oxidation promoted by hematite nanoparticles. *Geochim. Cosmochim. Acta* **2005**, *69*, 389−398.
(68) Villalobos, M.; Carrillo-Cárdenas, M.; Gibson, R.; López-Santiago, N. R.; Morales, J. A. The influence of particle size and structure on the sorption and oxidation behaviour of birnessite: II. Adsorption and oxidation of four polycyclic aromatic hydrocarbons. *Environ. Chem.* **2014**, *11*, 279−288.
(69) Liu, R.; Liu, H.; Qiang, Z.; Qu, J.; Li, G.; Wang, D. Effects of calcium ions on surface characteristics and adsorptive properties of hydrous manganese dioxide. *J. Colloid Interface Sci.* **2009**, *331*, 275−280.
(70) Huangfu, X.; Jiang, J.; Ma, J.; Liu, Y.; Yang, J. Aggregation kinetics of manganese dioxide colloids in aqueous solution: influence of humic substances and biomacromolecules. *Environ. Sci. Technol.* **2013**, *47*, 10285−10292.
(71) Morgan, J. J.; Stumm, W. Colloid-chemical properties of manganese dioxide. *J. Colloid Sci.* **1964**, *19*, 347−359.
(72) Costa, R. C. C.; Lelis, M. d. F. F.; Oliveira, L. C. A.; Fabris, J. D.; Ardisson, J. D.; Rios, R. R. V. A.; Silva, C. N.; Lago, R. M. Remarkable effect of Co and Mn on the activity of Fe3− xMxO4 promoted oxidation of organic contaminants in aqueous medium with H_2O_2. *Catal. Commun.* **2003**, *4*, 525−529.
(73) Costa, R.; Lelis, M.; Oliveira, L.; Fabris, J.; Ardisson, J.; Rios, R.; Silva, C.; Lago, R. Novel active heterogeneous Fenton system based on Fe3− xMxO4 (Fe, Co, Mn, Ni): the role of M2+ species on the reactivity towards H2O2 reactions. *J. Hazard. Mater.* **2006**, *129*, 171−178.
(74) Zhang, T.; Zhang, D.; Han, X.; Dong, T.; Guo, X.; Song, C.; Si, R.; Liu, W.; Liu, Y.; Zhao, Z. Preassembly Strategy To Fabricate Porous Hollow Carbonitride Spheres Inlaid with Single Cu−N3 Sites for Selective Oxidation of Benzene to Phenol. *J. Am. Chem. Soc.* **2018**, *140*, 16936−16940.
(75) Post, J. E. Manganese oxide minerals: Crystal structures and economic and environmental significance. *Proc. Natl. Acad. Sci. U.S.A.* **1999**, *96*, 3447−3454.
(76) Manceau, A.; Lanson, B.; Drits, V. A. Structure of heavy metal sorbed birnessite. Part III: Results from powder and polarized extended X-ray absorption fine structure spectroscopy. *Geochim. Cosmochim. Acta* **2002**, *66*, 2639−2663.
(77) Zhu, M.; Ginder-Vogel, M.; Parikh, S. J.; Feng, X.-H.; Sparks, D. L. Cation Effects on the Layer Structure of Biogenic Mn-Oxides. *Environ. Sci. Technol.* **2010**, *44*, 4465−4471.
(78) Golden, D. C.; Chen, C. C.; Dixon, J. B. Synthesis of Todorokite. *Science* **1986**, *231*, 717−719.
(79) Lefkowitz, J. P.; Elzinga, E. J. Structural alteration of hexagonal birnessite by aqueous Mn(II): Impacts on Ni(II) sorption. *Chem. Geol.* **2017**, *466*, 524−532.
(80) Li, Y.; Liu, F.; Xu, X.; Liu, Y.; Li, Y.; Ding, H.; Chen, N.; Yin, H.; Lin, H.; Wang, C.; Lu, A. Influence of heavy metal sorption pathway on the structure of biogenic birnessite: Insight from the band structure and photostability. *Geochim. Cosmochim. Acta* **2019**, *256*, 116−134.
(81) Nguyen, C. K.; Powers, K. A.; Raetz, M. A.; Parks, J. L.; Edwards, M. A. Rapid free chlorine decay in the presence of $Cu(OH)_2$: Chemistry and practical implications. *Water Res.* **2011**, *45*, 5302−5312.
(82) Pham, A. N.; Xing, G.; Miller, C. J.; Waite, T. D. Fenton-like copper redox chemistry revisited: hydrogen peroxide and superoxide mediation of copper-catalyzed oxidant production. *J. Catal.* **2013**, *301*, 54−64.
(83) Meyerstein, D. Trivalent copper. I. Pulse radiolytic study of the chemical properties of the aquo complex. *Inorg. Chem.* **1971**, *10*, 638−641.
(84) Ulanski, P.; von Sonntag, C. Stability Constants and Decay of Aqua-Copper (III)−A Study by Pulse Radiolysis with Conductometric and Optical Detection. *Eur. J. Inorg. Chem.* **2000**, 1211−1217.

https://dx.doi.org/10.1021/acs.est.9b06497
Environ. Sci. Technol. 2020, 54, 1963−1972